Conformational Analysis of l-(Alkoxymethyl)-5(*R*)-methyl-2-pyrrolidinone Derivatives. Determination of the Absolute Stereochemistry of Alcohols

Shamil K. Latypov,*,† Ricardo Riguera,‡ Michael B. Smith,*,§ and Jana Polivkova§

The Institute of Organic and Physical Chemistry of Russian Academy of Sciences, Kazan, 420083, Tatarstan Republic, the Russian Federation, Departamento de Quimica Organica, Facultad de Quimica, Universidad de Santiago de Compostela, 15706, Santiago de Compostela, Spain, and Department of Chemistry, University of Connecticut, 55 N. Eagleville Road, 4-60, Storrs, Connecticut 06269-3060

Received January 6, 1998

Parameters that allow prediction of the sense of NMR nonequivalence in *N*-(alkoxymethyl)-2-pyrrolidinone derivatives (**2**−**8**) are identified. These derivatives are prepared by the reaction of chiral racemic and chiral nonracemic alcohols with 1-(chloromethyl)-5(*R*)-methyl-2-pyrrolidinone, **1**. The factors governing NMR nonequivalence ($\Delta\delta$) in **2**−**8** were first established. The NMR parameters were then determined and compared with those derived from calculated conformations for **2**−**8**. This information was used to establish the absolute stereochemistry of the alcohol adducts.

Introduction

An important part of modern organic chemistry is the development of stereospecific or highly stereoselective reactions. These reactions generate compounds enriched in one enantiomer, but they are not usually enantiopure, so determining the enantiomeric composition of these compounds is important. There are several methods available for this purpose, including chiral-phase HPLC. An alternative approach treats an enantiomeric mixture with one of many derivatizing agents that can be used in conjunction with NMR. Perhaps the most commonly used agent is α-methoxy-α-(trifluoromethyl)phenylacetic acid, known as Mosher's acid (MTPA).[1] This acid reacts with alcohols or amines to form so-called Mosher's esters or Mosher's amides. These derivatives contain the chiral center from MTPA as well as the one(s) from the chiral alcohol or amine, generating diastereomeric esters or amides that can be distinguished by either proton or fluorine NMR. The success of this method relies on differences in the NMR parameters of the diastereomers. The NMR method can be used to determine enantiomeric composition only if the enantiomers, indistinguishable in terms of their NMR, can be transformed into diastereomers whose NMR signals can be distinguished.

In those cases where the derivatizing agent or the chiral substrate contains an aryl ring linked to the chiral center, a model has been developed to realize the sense of nonequivalence in the NMR. In this model, the two factors controlling nonequivalence are aromatic shielding effects[2] and the conformational preference of the aryl-methoxyacetic ester.[3] There is a straightforward correlation between these NMR parameters and the structure of the ester that allows prediction of the absolute stereochemistry.

To date, esters and amides derived from MTPA are the only examples that do not involve aromatic shielding effects,[1b,4] and these are usually analyzed by ^{19}F NMR spectroscopy. According to a "static" model used for MTPA derivatives, the difference in chemical shifts arises from the anisotropy effect of the carbonyl bond which is due to distortions in the geometry of the respective diastereomers. The value of this model has been called into doubt since the conformational equilibrium of MTPA esters is complex.[5] The model used to explain anisotropy effects of a carbonyl bond has been revised.[6]

Several new reagents have been reported that react with alcohols to generate diastereomeric mixtures and allow the enantiomeric excess (%ee) of the original alcohol to be determined.[7] Although effective for determining %ee, no attempt was made to develop approaches to find the absolute stereochemistry of the alcohols from the NMR parameters of the derivatives. The main obstacles are the precision of the NMR theory and the complexity of the presumed conformational equilibrium for each molecule. Among the recently reported reagents, 5(*R*)-methyl-l-(chloromethyl)-2-pyrrolidinone (**1**)[8] is particularly interesting. It reacts with alcohols to give adducts that exhibit simple ^{1}H NMR spectra for the diastereotopic

† The Institute of Organic and Physical Chemistry of Russian Academy of Sciences. Email: slatypov@ksu.ru.

‡ Universidad de Santiago de Compostela. Fax 34-81-591091.

§ University of Connecticut. Email: smith@nucleus.chem.uconn.edu.

(1) (a) Dale, J. A.; Dull, D. L.; Mosher, H. S. *J. Org. Chem.* **1969**, *34*, 2543. (b) Dale, J. A.; Mosher, H. S. *J. Am. Chem. Soc.* **1973**, *95*, 512−519.

(2) (a) Waugh, J. S.; Fessenden, R. W. *J. Am. Chem. Soc.* **1957**, *79*, 846−849. (b) Johnson. C. E.; Bovey, F. A. *J. Chem. Phys.* **1958**, *29*, 1012−1014. (c) Jonathan, N.; Gordon, S.; Dailey, B. P. *J. Chem. Phys.* **1962**, *36*, 2443−2448. (d) Barfield. M.; Grant, D. M.; Ikenberry, D. *J. Am. Chem. Soc.* **1975**, *97*, 6956−6961. (e) Agarwal, A.; Barnes, J. A.; Fletcher, J. L.; McGlinchey, M. J.; Saver, B. G. *Can. J. Chem.* **1977**, *55*, 2575−2581. (f) Haigh, C. W.; Mallion, R. B. *Prog. NMR Spectrosc.* **1980** *13*, 303−344.

(3) Latypov, Sh. K.; Seco, J. M.; Quinoa, E.; Riguera, R. *J. Org. Chem.* **1995**, *60*, 504−515.

(4) (a) Ohtani, I.; Kusumi, T.; Kashman, Y.; Kakisawa, H. *J. Am. Chem. Soc.* **1991**, *113*, 4092−4096. (b) Rieser, M.; Hui, Y.; Rupprecht, J. K.; Kozlowski, J. F.; Wood, K. V.; McLaughlin, J. L.; Hanson. P. R.; Zhuang, Z.; Hoye, T. R. *Ibid.* **1992**, *114*, 10203−10213. Yu, J.-G.; Hu, X.; Ho, D.; Bean, M. F.; Stephens, R. E.; Cassady, J. M. *J. Org. Chem.* **1994**, *59*, 1598−1599.

(5) Latypov, Sh. K.; Seco, J. M.; Quinoa, E.; Riguera, R. *J. Org. Chem.* **1996**, *61*, 8569−8577.

(6) (a) Karabatsos, G. J.; Hsi, N. *J. Am. Chem. Soc.* **1965**, *87*, 2864−2870. (b) ApSimon, J. W.; Whalley, W. B. *Chem. Commun.* **1966**, 754−755. (c) Karabatsos, G. J.; Sonnichsen, G. C.; Hsi, N.; Fenoglio, D. J. *J. Am. Chem. Soc.* **1967**, *89*, 5067−5068. (d) Balasubrahamanyam, S. N.; Bharathi, S. N.; Usga, G. *Org. Magn. Reson.* **1983**, *21*, 474−481.

10.1021/jo980029+ CCC: $15.00
Published on Web 11/06/1998

Chart 1

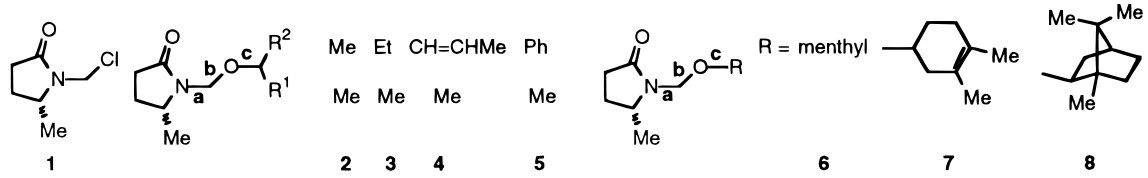

Chart 2

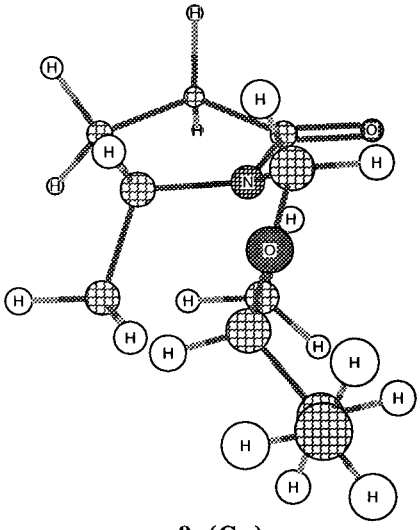

9 (G+)

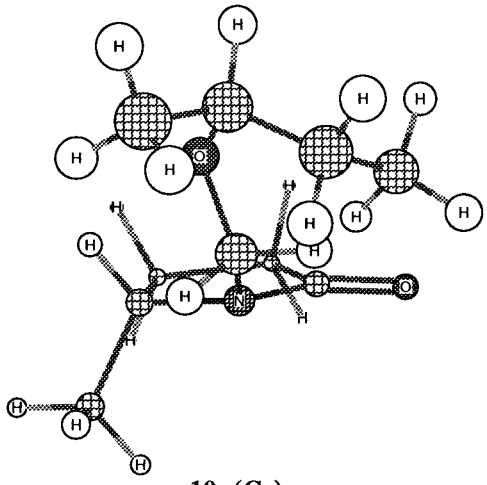

10 (G-)

NCH_2OR protons. The NCH_2O signals are not coupled with other protons of either the lactam or the alcohol, and they appear in a region of the ^{1}H NMR spectrum that makes them ideal for analysis. Integration allows one to determine the enantiomeric composition of the starting alcohol. Such analysis would be useful for a series of alcohols requiring rapid analysis or when it is important to determine if one member of a series has the same configuration as the others.

Analysis based on derivatives of **1** would be more useful if the sense of nonequivalence in diastereomers such as **2**−**8** could be predicted (Chart 1). These NMR parameters (usually expressed as $\Delta\delta$) must be determined before we can establish a model that will predict the absolute stereochemistry. In this work, we predict the conformational preferences of alcohol adducts **2**−**8**, and this allows us to generate a model to predict the absolute stereochemistry of the parent alcohols. Both the advantages and limitations of this method are discussed.

Results and Discussion

Before deriving a model, we must determine the origin of nonequivalence in the proton NMR for diastereomers **2**−**8** (*R*,*S*). If we focus on structure **2** (the adduct derived from 2-propanol where $R^1 = R^2 =$ Me), rotation about bonds a, b, and c will lead to different rotamers that will exist in equilibrium for each diastereomer. For a given diastereomer, rotation about the N−C bond (bond a) will lead to two important rotamers (G+ and G−, see Figure 1). Conformations G+ and G− are slightly different in energy due to greater steric interactions with the C_5 methyl group of the pyrrolidinone ring in G+. The G+ conformation for the (2*S*)-butanol adduct is represented as **9**, and the G− conformation for the (2*S*)-butanol adduct is represented as **10**. There is a steric interaction between the alkoxymethyl unit in **9** (G+) and the methyl group, but this is missing in **10** (G−) since those groups have an anti-orientation (Chart 2). In this representation, the five-membered 2-pyrrolidinone ring is assumed to be relatively flat rather than having an "envelope" shape, with the methyl group at C_5 projected toward the "bottom" of that ring. When compared with **9** and **10**, the simplistic models in Figure 1 are reasonable representations for G+ and G−.

The diastereotopic protons of the N−CH_2−O unit, H_a and H_b in Figure 1, should be intrinsically nonequivalent, but if $R^1 = R^2$ then the energies of G− and G+ are close in energy. In G− proton H_a is shielded by the anisotropy effect of the lactam carbonyl, so it will resonate upfield. If this is correct, then H_a in G+ will be downfield with H_b shielded by the carbonyl. This is entirely consistent with experimental observations made for adducts **2**−**8**, and the observed nonequivalence reflects a small excess of the lower energy G− conformer. When R^1 and R^2 are identical ($R^1 = R^2 =$ Me in **2**), the NMR spectrum is the symmetrical AB pattern shown in Figure 1. When R^1 and R^2 are different, the energy difference between G− and G+ leads to nonequivalence for H_a and H_b. The effect

(7) (a) Takeuchi, Y.; Itoh, N. Note, H.; Koizumi, T.; Yamaguchi, K. *J. Am. Chem. Soc.* **1991**, *113*, 6318−6320. (b) Trujillo, M.; Morales, E. Q.; Vazquez, J. T. *J. Org. Chem.* **1994**, *59*, 6637−6642. (c) Fukushi, Y.; Yajima, C.; Mizutani, J. *Tetrahedron Lett.* **1994**, *35*, 599−602. (d) Fukushi, Y.; Yajima, C.; Mizutani, J. *Ibid.* **1994**, *35*, 8809−8812. (e) Fukushi, Y.; Yajima, C.; Mizutani, J. *Ibid.* **1994**, *35*, 9417−9420. (f) Oshikawa, T.; Yamashita, M.; Kumagai, S.; Seo, K.; Kobayashi, J. *J. Chem. Soc. Chem. Commun.* **1995**, 435−436. (g) Peng, J.; Barr, M. E.; Ashburn, D. A.; Lebioda, L.; Garber, A. R.; Martinez, R. A.; Odom, J. D.; Dunlap, R. B.; Silks, L. A. *J. Org. Chem.* **1995**, *60*, 5540−5549. (h) Wu, R.; Odom, J. D.; Dunlap, R. B.; Silks, L. A. *Tetrahedron Asymmetry* **1995**, *6*, 833−834. (i) Hulst, R.; Kellogg, R. M.; Feringa, B. *Recl. Trav. Chim. Pays-Bas* **1995**, *114*, 115−138.

(8) Smith, M. B.; Dembofsky, B. T.; Son, Y. C. *J. Org. Chem.* **1994**, *59*, 1719−1725.

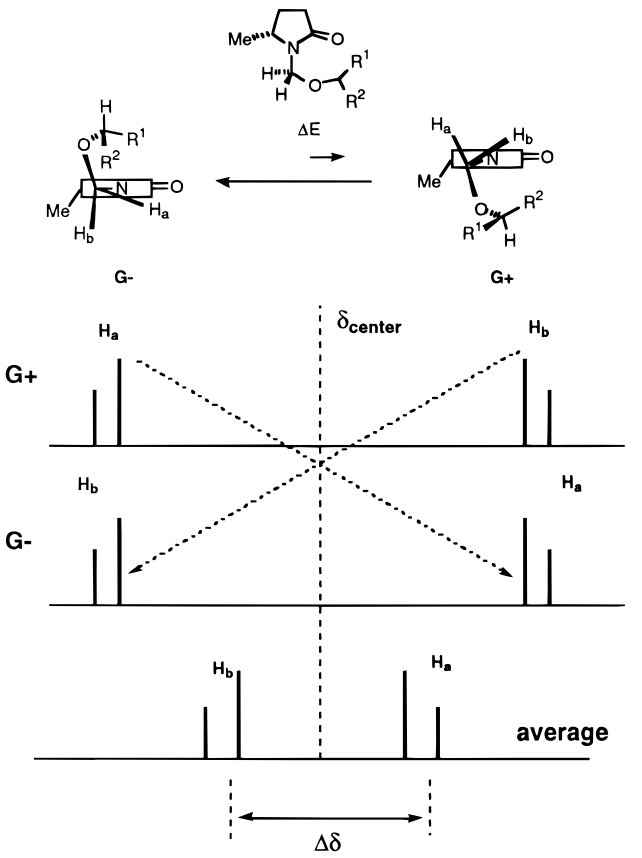

Figure 1. The unique set of conformations (G+ and G−) for diastereomers formed by the reaction of **1** with alcohols having at least one chiral center.

is different for the (*R*)- and (*S*)-adducts, which is the basis for differentiating the two diastereomers.

When comparing adducts of **1** derived from (*R*) vs (*S*) alcohols we must take into account the (*R*)-chiral center at C_5 of the lactam, which influences the intrinsic conformational preference of each diastereomer.

These interactions were noted for the (2*S*)-butanol adduct in **9** and **10**. Changing the absolute configuration of the chiral center in the alcohol precursor will redistribute the ground state conformer population in the adduct (see Figure 2). The intrinsic chirality of the alcohol moiety, chemical shift, and the interactions which lead to variation in ground state conformations are all related. This hypothesis is strongly supported by the following facts. The NCH_2O protons generate AB-like spectra, and the centers of AB are at virtually the same place ($\delta = 4.76-4.80$). In compounds **3**−**6** and **8**, which have different R^1 and R^2 groups and are more hindered from one side of the chiral center, the difference between $\Delta\delta(R)$ and $\Delta\delta(S)$ is larger. In **2**, R^1 and R^2 are the same and in **7** "R^1" and "R^2" are part of cyclohexene ring where the alkene and methyl units are removed from C_α. In both cases, $\Delta\delta(R) = \Delta\delta(S)$. In Figure 2, both the "R" and "S" adducts show a preference for G− due to steric interactions. Each rotamer will generate an AB signal based on the magnitude of ΔE (E_{G-} vs E_{G+}). If ΔE for the "R" adduct is greater than ΔE for the "S" adduct, the result is the NMR signal shown in Figure 2. This is an attractive model, but the important question is whether it can be used to predict enantiomeric composition of the alcohol precursor. We must verify that the structure and energies of the main conformers are consistent with our prediction. We turned to calculations.

Conformational Analysis

We first used a molecular mechanics (MM) simulation (pc91 force field) to probe conformational variations in alcohol adducts of **1**. The interaction of the oxygen atom in the $N-CH_2-O$ unit with the lactam carbonyl group led to two minimum energy orientations around the N−C bond, described above as rotamers G+ and G− (see **9** and **10**). Two additional conformers were obtained by rotation about C−O bonds (nonlinear, $N-C-O-C = 90°$ and linear, $N-C-O-C \approx 180°$), shown in Figure 3. They can also be seen on the energy contour map obtained by rotation around the N−C and C−O bonds (see Figure 4), where there are four minima. Inversion of the five-membered lactam ring doubles the number of conformers (i.e., the C_5 methyl can be pseudoaxial or pseudoequatorial). The terms pseudoaxial and pseudoequatorial are used to describe the position of the methyl group in a planar five-membered lactam ring and an "envelope" lactam ring, respectively. This leads to the assumption that compounds **2**−**8** exist in an equilibrium with at least eight conformers. For each pair of G+ and G− conformers, there is almost always a preference for the G− form (0.2−0.5 kcal/mol for **2**, see Table 1) due to the steric interaction of the methyl group with the alkoxyalkyl group in G+. In **9** and **10**, the positions of the NCH_2O protons are quite similar, however, suggesting that their magnetic environments are similar.

Analysis by semiempirical methods (AM1 and PM3) also shows that there is a preference for the G− rotamer. Unlike the molecular mechanics simulation, the AM1 and PM3 analyses suggest that the "linear" conformers ($N-C-O-C = 180°$) are higher in energy than the "nonlinear" conformers. During the minimization, both methods showed an energy minimum corresponding to "nonlinear" forms (that is why two semiempirical methods were used). The AM1 analysis predicts an energy gap that favors G− by about 0.14 kcal/mol for **2**.

We wanted to determine the validity of the theoretical predictions with an experimental method. Dynamic NMR (DNMR) appeared to be the best choice since it was compatible with detecting the thermodynamic parameters of the equilibrium and the geometry of the conformers, while retaining the possibility of detecting anisotropy effects for the carbonyl and aryl fragments. In our analysis, decreasing the temperature led to an increase of nonequivalence for the CH_2 protons ($\Delta\delta$) in *almost* all cases (see Table 2). This corresponds to an increase in the population of the low energy conformer and, hence, its contribution to average NMR parameters. This observation was consistent with the theoretical predictions.

Anomalous behavior was observed for the menthyl derivative (*S*)-**6** for reasons that we cannot yet explain. At low temperatures, the magnitude of $\Delta\delta$ was diminished, and two broad lines were obtained for the CH_2 protons. Moreover, these signals collapsed to a broad singlet at $\delta = 4.710$ ($T = 173$ K) when the experiment was carried out in acetone solution (see Table 2).[9] This is probably due to steric hindrance from one side that

(9) This fact is also in agreement with theory. The geometry of menthol is such that it is hindered from one side, destabilizing the G− form in the adduct from the *S* enantiomer (see Table 1). This can be seen on the energy contour map (see Figure 5). The linear conformer is more stable, and the barrier to interconversion (G+G−) is higher. The menthol adduct prefers a linear structure.

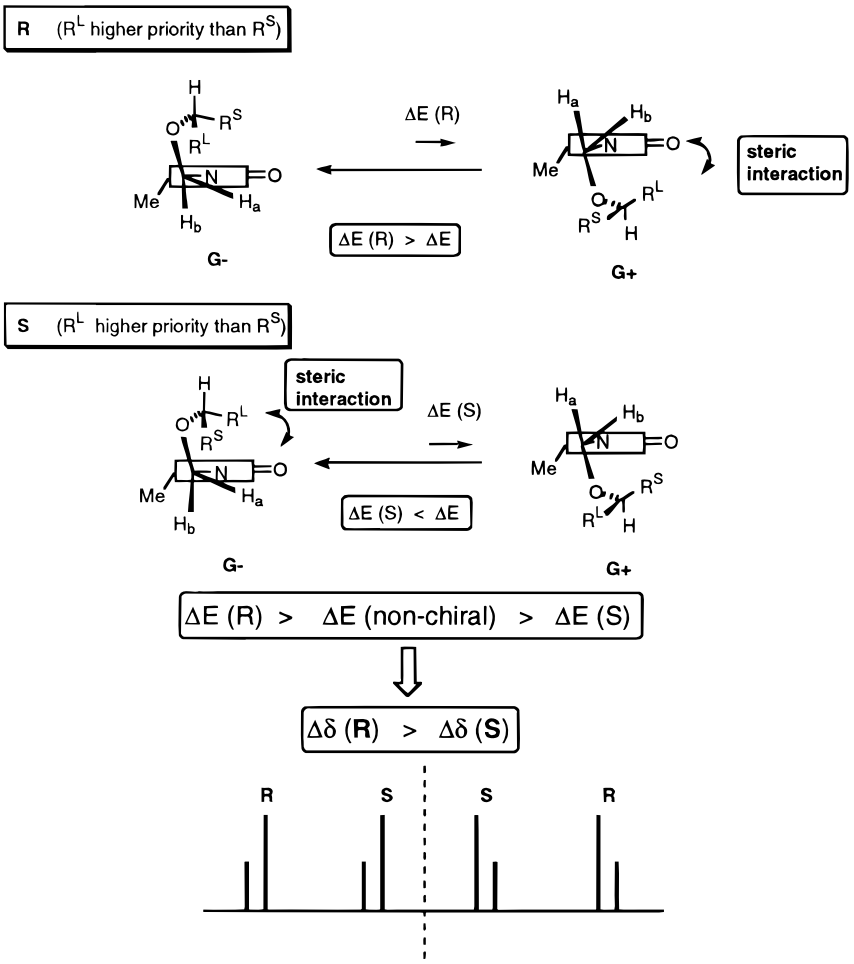

Figure 2. Intrinsic differences in conformational preference for adducts derived from different diastereomers of **1** and alcohols having a chiral center.

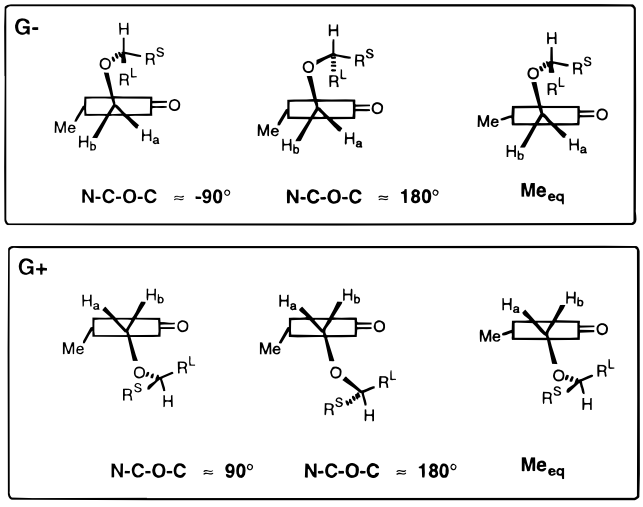

Figure 3. G+ and G− orientations; nonlinear, N−C−O−C = 90° and linear, N−C−O−C ≈ 180° compared to the relative position of the C_5 methyl group.

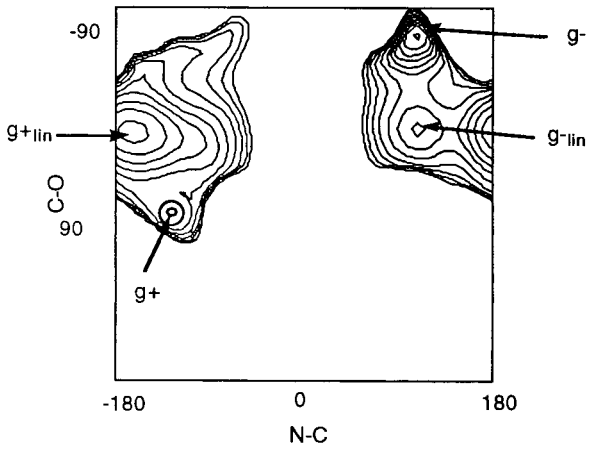

Figure 4. Energy contour map for rotation about the N−C and C−O bonds in **2**.

destabilizes the G− form in the adduct from the S enantiomer as seen on the energy contour map in Figure 5).

Since the l-phenylethanol derivatives **5** (*R* and *S*) have a phenyl unit, we used a complimentary analysis to detect the aromatic shielding increments. Detailed analysis of the proton NMR spectra of (*R*)-**5** and (*S*)-**5** showed remarkable shielding and deshielding effects relative to **2**, in $CDCl_3$. As shown in Table 3, in (*R*)-**5**, H_5 showed signals at $\delta = 3.412$ (vs $\delta = 3.700$ in **2**), H_{4eq} showed signals at $\delta = 1.322$ (vs $\delta = 1.527$), H_{4ax} at $\delta = 1.698$ (vs $\delta = 2.140$), H_{3eq} at $\delta = 1.826$ (vs $\delta = 2.214$), H_{3ax} at $\delta = 2.107$ (vs $\delta = 2.294$), and lower values for the C_5 Me ($\delta = 1.15$ vs $\delta = 1.233$ in **2**). In (*S*)-**5** the primary differences were for signals corresponding to the C_5 Me at $\delta = 1.143$ (vs $\delta = 1.233$ in **2**), H_{3ax} at $\delta = 2.255$ (vs $\delta = 2.294$), and H_{4eq} at $\delta = 1.497$ (vs $\delta = 1.527$). In Table 3, the term s_{eff}

Table 1. Molecular Modeling (MM)[a] Calculations for Adducts 2−8

comp	config	conform	E_{ax}[b]	E_{eq}	E_{ax_lin}	ΔE(G+, G−)[c]	$\Delta\delta_{AB}$[d]
2		G+	−47.22	−46.30	−47.57		
		G−	−47.48	−46.83	−47.95	0.26	0.334[e]
3	*R*	G+	−43.33	−42.41	−43.71		
		G−	−43.75	−43.09	−44.12	0.42	0.54[f]
	S	G+	−43.48	−42.56	−43.61		
		G−	−43.61	−42.95	−44.07	0.13	0.44[f]
4	*R*	G+	−41.26	−40.35	−41.35		
		G−	−41.72	−40.34	−41.68	0.46	0.73[f]
	S	G+	−41.26	−39.73	−41.28		
		G−	−41.52	−40.85	−41.73	0.26	0.15[f]
5	*R*	G+	−27.66	−26.76	−27.97		0.50[f]
		G−	−28.80	−28.09	−28.21	1.14	0.364[e]
	S	G+	−27.88	−27.20	−27.79		0.42[f]
		G−	−27.91	−27.24	−28.30	0.03	0.465[e]
6	*R*	G+	−59.61	−58.81	−60.62		0.80[f]
		G−	−60.93	−60.14	−60.62	1.32	0.722[e]
	S	G+	−60.34	−59.56	−60.20		0.44[f]
		G−	−59.92	−59.77	−60.51	−0.42	0.263[e]
7	*R*	G+	−40.74	−39.87	−41.16		
		G−	−40.95	−40.31	−41.41	0.21	0.32[f]
	S	G+	−40.74	−39.87	−41.16		
		G−	−40.95	−40.31	−41.41	0.21	0.32[f]
8	*R*	G+	−38.19	−37.55	−39.04		
		G−	−38.92	−38.28	−39.23	0.73	0.47[f]
	S	G+	−38.53	−37.71	−38.98		
		G−	−38.69	−38.03	−39.39	0.16	0.39[f]

[a] With pcff91 force field. [b] In kcal/mol. [c] ΔE(G+, G−) = E_{ax}(G+) − E_{ax}(G−). [d] In ppm. [e] In CS_2 + CD_2Cl_2. [f] In $CDCl_3$.

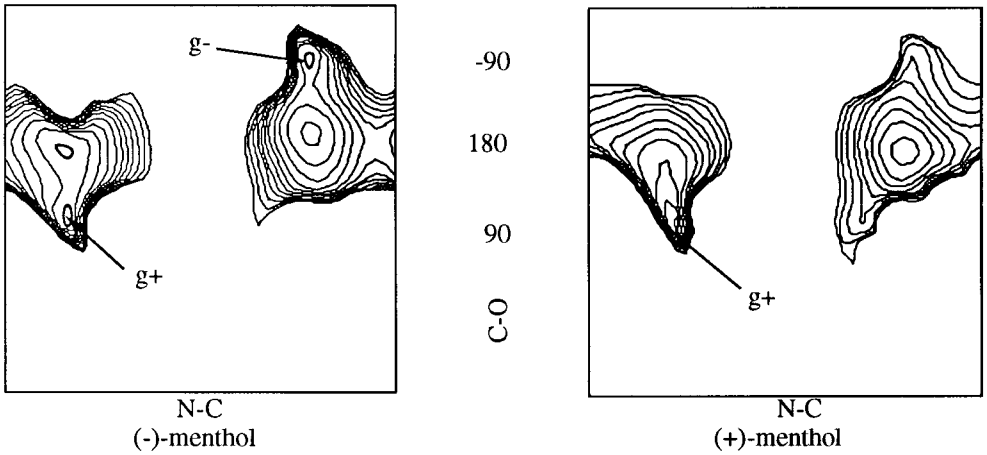

Figure 5. Contour maps of the energy as a function of the N−C and C−O angles for (−) and (+)-menthol adducts.

Table 2. ^{1}H NMR Parameters for Adducts 2−8 (in $CDCl_3$, CS_2, and acetone)

alcohol (solvent, temp)	δ_A	δ_B	δ_{center}	$\Delta\delta_{AB}$
2 (CS_2, 300 K)	4.78	4.45	4.61	0.33
2 (CS_2, 176 K)	4.87	4.40	4.64	0.48
(*R*)-**3** ($CDCl_3$, 300 K)	5.04	4.50	4.77	0.54
(*S*)-**3** ($CDCl_3$, 300 K)	4.98	4.55	4.77	0.44
(*R*)-*t*-**4**[a] ($CDCl_3$, 300 K)	5.06	4.33	4.70	0.73
(*S*)-*t*-**4**[a] ($CDCl_3$, 300 K)	4.72	4.57	4.65	0.15
(*R*)-**5** ($CDCl_3$, 300 K)	5.02	4.52	4.77	0.50
(*S*)-**5** ($CDCl_3$, 300 K)	4.92	4.50	4.71	0.42
(*R*)-**5** (CS_2, 300 K)	4.78	4.42	4.60	0.36
(*R*)-**5** (CS_2, 213 K)	4.78	4.35	4.57	0.43
(*S*)-**5** (CS_2, 300 K)	4.73	4.26	4.50	0.47
(*S*)-**5** (CS_2, 213 K)	4.71	4.19	4.45	0.51
(*R*)-**6** ($CDCl_3$, 300 K)	5.18	4.38	4.78	0.80
(*S*)-**6** ($CDCl_3$, 300 K)	4.99	4.55	4.77	0.44
(*R*)-**6** (CS_2, 300 K)	4.98	4.26	4.62	0.72
(*R*)-**6** (CS_2, 181.5 K)	5.07	4.14	4.61	0.93
(*S*)-**6** (CS_2, 300 K)	4.74	4.48	4.61	0.26
(*S*)-**6** (CS_2, 163 K)	4.73	4.51	4.62	0.21
(*R*)-**6** (acetone, 300 K)	5.05	4.39	4.72	0.66
(*R*)-**6** (acetone, 177 K)	5.12	4.31	4.72	0.81
(*S*)-**6** (acetone, 300 K)	4.85	4.58	4.72	0.27
(*S*)-**6** (acetone, 163 K)	4.71	4.71	4.71	0
(*R*)-**7** ($CDCl_3$, 300 K)	4.92	4.60	4.76	0.32
(*S*)-**7** ($CDCl_3$, 300 K)	4.92	4.60	4.76	0.32
(*R*)-**8** ($CDCl_3$, 300 K)	4.93	4.46	4.70	0.47
(*S*)-**8** ($CDCl_3$, 300 K)	4.91	4.52	4.72	0.39

[a] For **4**, *t*-**4** = *trans*-**4**

is used for shielding effects. In addition, low-temperature experiments showed that shielding increments increased (up to 1.5−2 times) in (*R*)-**5**, in full agreement with the conformational model (see Table 3), but these small shielding increments almost vanished in the (*S*)-**5** diastereomer. Notable deshielding contributions were detected that corresponded to the effects predicted for the low energy conformer (see Table 3, last column). For simplicity, only increments for the axial conformer were calculated.

Calculation of the shielding effects and comparison with experimental values (Table 3) strongly support the premise that G+ and G− are the main conformations in both diastereomers, with angles for N−C−O−C_a of 80−90°. Good correlation between theoretical and experimental shielding increments was obtained for the diastereotopic NCH_2O protons in the compounds that were analyzed (see Table 1). This led to two conclusions. First, those conformers with a linear orientation of the N−C−O−C bond, which does not lead to shielding, are less stable. Molecular mechanics calculations slightly overestimated the stability of these "linear" conformers. Second, the planar conformation dominates for the five-

Table 3. Chemical Shifts of Ring Protons in 2, (*R*)-5, and (*S*)-5 (in ppm, CS_2 + CD_2Cl_2, 75%/25% Solvent). Experimental and Theoretical Shielding Increments ($\Delta\sigma$, in ppm)[a] of the Aryl Ring in (*R*)-5 and (*S*)-5 in Shielding-Producing Conformations

	chem shifts (ppm)														
	2	2	(*R*)-**5**	(*R*)-**5**	(*S*)-**5**	(*S*)-**5**	s_{eff} (exp) (*R*)-**5**		s_{eff} (exp) (*S*)-**5**		s_{eff} (predicted) (*R*)-**5**[b]		s_{eff} (predicted) (*S*)-**5**[c]		
proton	300 K	176 K	300 K	213 K	300 K	177 K	300 K	213 K	300 K	177 K	ax	eq	ax	ax	eq
3eq	2.21	2.35	1.83	1.59	2.26	2.44	0.39	0.76	−0.04	−0.09	0.48	1.28	0.16	−0.06	0.22
3ax	2.29	2.35	2.11	2.00	2.26	2.37	0.19	0.35	0.04	−0.02	0.28	0.34	0.57	−0.02	0.39
4eq	1.53	1.58	1.32	1.17	1.50	1.59	0.21	0.41	0.03	−0.01	0.51	0.27	0.28	−0.03	1.29
4ax	2.14	2.19	1.70	1.37	2.15	2.25	0.44	0.83	−0.01	−0.06	1.94	0.47	0.16	−0.07	0.39
5	3.70	3.73	3.41	3.26	3.75	3.84	0.29	0.47	−0.05	−0.11	0.42	0.54	0.18	−0.07	0.22
Me-5	1.23	1.25	1.15	1.09	1.14	1.20	0.08	0.16	0.09	0.05	0.15	0.11	0.80	0.00	0.24

[a] s_{eff} = shielding effects. Calculated as $\Delta\sigma = \delta(\mathbf{5}) - \delta(\mathbf{2})$. [b] G− conformer. [c] G+ conformer.

membered lactam ring, where the methyl group at C_5 is pseudoaxial. The envelope conformation having a pseudoequatorial methyl is less populated.

Nonequivalence of the NCH_2O protons can be explained by the shielding effect of the C=O group (the inplanar proton) and also by polar effects of the N−CH_2−O oxygen atom. A low field shift corresponds to the signal from an out of planar proton that is, in this case, coplanar with the C−O bond (angle = 153°). The AM1 calculation predicted a charge difference ($\Delta\epsilon^*$ = 0.01−0.02) that corresponds to $\Delta\delta$ = 0.27−0.54.

Determining Absolute Stereochemistry. With the ground state conformations established, we determined the chirality−NMR parameter relationships. Bulky alkyl groups (marked R^L) should destabilize G+ in the *R*-alcohol diastereomer and G− in the *S*-alcohol diastereomer. The calculated energy of the main conformers of **3**, **5**, and **6** (see Table 1) shows that the energy difference is higher for the diastereomer derived from the *R*-enantiomer. This energy difference modifies the populations of the conformers and, hence, the average NMR parameters ($\Delta\delta$). This demonstrates a direct relationship between the absolute stereochemistry, energy difference, and the NMR parameters. As can be seen from Tables 1 and 2 of the (*R*) vs the (*S*) enantiomer, a higher energy difference corresponds to higher NMR nonequivalence.[10] The NCH_2O protons in (*S*)-**5**, for example, are affected by the shielding/deshielding effects of the aryl ring in a different manner in the respective conformers in *R* and *S* (see Figure 6). In the *sec*-butanol derivative (**3**), (*R*)-**3** showed signals at δ = 5.04 and δ = 4.50, whereas (*S*)-**3** showed those signals at δ = 4.98 and δ = 4.55. The menthol adduct **6** showed signals at δ = 5.18 and δ = 4.38 for (*R*)-**6** and at δ = 4.99 and δ = 4.55 for (*S*)-**6**.

In diastereomers derived from the *R*-enantiomer, small deshielding effects are expected in G−. Therefore, anisotropic effects of the carbonyl bond and polar effects of the vicinal oxygen are the main parameters that will determine the value of $\Delta\delta_{AB}$. In diastereomers derived from (*S*)-enantiomers, there is a notable increase of $\Delta\delta_{AB}$ (up to δ = 0.44 in **6**) with respect to those derived from (*R*)-enantiomers. Therefore, a high field shift of δ_{center} (up to about δ = 0.27) is expected in G−. This explains both the higher $\Delta\delta_{AB}$ observed in the adduct derived from enantiopure (*S*)-alcohol and the high field shift of δ_{center},

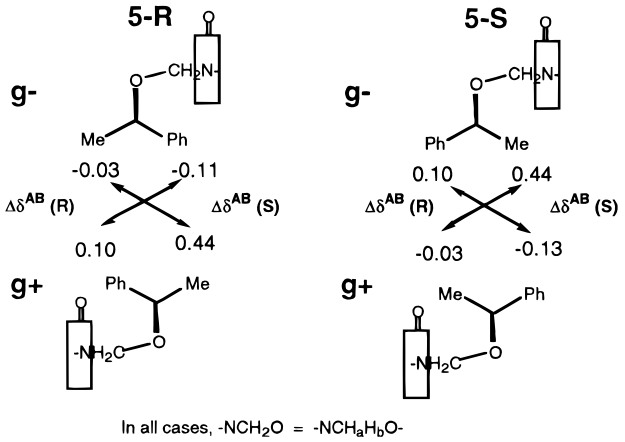

Figure 6. Shielding/deshielding increments due to anisotropy of the phenyl group, calculated for NCH_2O otons in two main low energy conformers of (*R*)-**5** and (*S*)-**5**.

which was observed to be as high as δ = 0.1. The good correlation of δ_{center} in other cases suggests that no additional contributions to the proton chemical shifts are required.

In the case of symmetrical alcohols, or where the chiral center is removed from the hydroxy-bearing carbon, the energy gap should not be changed or it should be changed in a similar manner for derivatives from both the (*R*) and (*S*) alcohols. In those cases, it should be difficult to differentiate the NMR signals from the (*R*)- and (*S*)-adducts (see **2** and **7**, $\Delta\delta_R = \Delta\delta_S$ entries in Table 1). To correlate NMR parameters with the absolute stereochemistry of the alcohol, we must compare energy differences between the two main conformers in both diastereomers. Our model suggests that the diastereomer with the higher energy difference should have NMR signals with greater nonequivalence ($\Delta\delta$), and both diastereomers must be prepared and analyzed. If only one enantiomer is present, determining the absolute configuration is difficult. In general, however, the proposed model works when there is a large group (R^L) relative to a small group (R^S) on the oxygen-bearing carbon of the adduct. The model predicts the absolute configuration of that carbon to have the largest $\Delta\delta$ for the (*R*) alcohol precursor, if the Cahn−Ingold−Prelog selection rules predict R^L to have a higher priority than R^S. A better understanding of the conformational preference of the molecule under study will require improvement in the resolution for the low-temperature NMR experiments.

(10) For (*S*)-**5** (in CS_2) dissimilar behavior was obtained due to additional anisotropic effect of an aryl ring on chemical shifts of NCH_2O protons [$\Delta\delta^{AB}$ (*S*) > $\Delta\delta^{AB}$ (*R*) although $\Delta E(R) < \Delta E(S)$]. According to calculations, these protons are affected by the shielding/deshielding effects of the aryl ring in a different manner in the respective conformers in *R* and *S* (see Figure 6). Figure 6 predicts small differences in the NMR behavior of **5**.

Conclusions

1. *N*-(Alkoxymethyl)-2-pyrrolidinone derivatives in solution exist in an equilibrium where two conformational forms predominate, G− and G+. These are generated by rotation of the CH_2OR unit about the C−N bond. In these forms, the lactam ring is essentially planar, and the C_5-methyl group has a pseudoaxial orientation. Therefore, the conformation with the NCOC angle of about 90° is lower in energy than the conformation with a linear arrangement (NCOC angle of about 180°).

2. The NMR parameters of the NCH_2O protons are determined by a combination of anisotropy effects of the C═O bond and polar effect of the oxygen. The most important contribution is the relative population of the two principal conformers.

3. These effects define the relationship between NMR parameters and absolute stereochemistry. Application of this model to a variety of derivatives (**2**−**8**) predicts the correct stereochemistry.

4. Simple computational methods can be correlated with the NMR spectra, and this method can be useful for determining the absolute stereochemistry of chiral alcohols that form adducts with lactam **1**.

Experimental Section

l-(Chloromethyl)-5(*R*)-methyl-2-pyrrolidinone (**1**) and alcohol adducts **3**−**8** were prepared by methods described by Smith.[8] Adduct **2** was prepared by the reaction of **1** with 2-propanol under standard conditions, as described below.

5(*R*)-Methyl-l-(isopropoxymethyl)-2-pyrrolidinone, 2. 2-Propanol (0.100 g, 1.35 mmol), sodium hydride (60% in mineral oil, 0.060 g, 1.5 mmol), and l-(chloromethyl)-5(*R*)-methyl-2-pyrrolidinone (**1**, 0.222 g, 1.50 mmol) were refluxed in dichloromethane for 1 h, and the crude material was purified as described in the literature[8] to yield 0.176 g (0.95 mmol, 70%) of **2** as a colorless liquid; R_f, 0.43 (diethyl ether, silica gel); ^{1}H NMR ($CDCl_3$): δ = 4.98 (d, J = 10.6 Hz, 1H), 4.55 (d, J = 10.6 Hz, 1H), 3.81 (m, 1H), 3.46 (m, 1H), 1.50 (m, 3H), 1.26 (d, J = 6.4 Hz, 3H), 1.15 (d, J = 6.0 Hz, 3H) and 0.88 (t, J = 7.5 Hz, 3H); ^{13}C NMR ($CDCl_3$): δ = 175.8, 74.8, 68.9, 52.7, 30.6, 29.1, 26.9, 19.9, 19.7, and 9.7 ppm; IR (neat, KBr): 3460, 2969, 1702, 1458, 1410, 1377, 1316 cm^{-1}; mass spectrum, *m*/*z*, (rel. intensity): 55 (21), 56 (14,), 57 (13), 83 (21), 84 (27), 98 (15), 100 (8), 112 (100), 113 (12), 128 (13), 156 (0.1, $M^+ - C_2H_5$); HRMS calcd for $C_8H_{14}NO_2$: *m*/*z* 156.1023, found 156.1024; $[\alpha]^{20}_D$ +5.4° (*c* = 0.093, $CHCl_3$).

Computational Methods. Molecular mechanics (MM, employing the pc91 force fields[11]) and AM 1 (PM3) were performed by the Insight II package on a Silicon Graphics Iris (SGI) computer. Initial molecular geometries originated from the Builder Module of Insight II; 3D coordinates were then generated from the bond lengths, bond angles and dihedral angles by the DG-II package.[12] The conformational space of each compound was scanned by MM optimization of the sterically allowed conformations around key single bonds. Some of the conformers were localized by means of gentle molecular dynamics (MD) simulations (T = 50 K). The MM and MD simulations were carried out in vacuo. Analysis of conformational transitions, identification of the low energy conformers, and calculation of the energy barriers between these conformers were all carried out by MM with an additional harmonic term of the form $k(l + \cos(nO\text{-}00))$ included in the force field. The energies of all conformations were minimized in Cartesian coordinate space by the block diagonal Newton−Raphson method; minima corresponded to rms energy gradients < 0.001 kcal/mol A. The ground-state energies of the geometries were then calculated by AM 1 (PM3) using the MOPAC 6.0 program. For all compounds, full geometry optimization was performed using the Broyden−Fletcher−Goldfarb−Shannon (BFGS) method and the PRECISE option.[13]

Shielding Effects. Calculations were carried out on a SGI computer by the program (written on Fortran 77) based to semiclassical model of Bovey and Johnson.[2] No corrections for local anisotropic contributions[2d,e] were implemented. π-Current loops separated by 1.39 Å.[2b,f]

NMR Spectroscopy. ^{1}H NMR spectra of samples in 4:1 CS_2/CD_2Cl_2 or $(CD_3)_2CO$ (ca. 2−3 mg in 0.5 mL) were recorded on a Bruker AMX 500 NMR spectrometer. Chemical shifts are reported in ppm (δ), internally referenced to the tetramethylsilane signal (δ = 0) in all cases. One- and two-dimensional NMR spectra were measured with standard pulse sequences. 2D Homo- (COSY) and heteronuclear (HMQC) shift correlation experiments were carried out using pulsed field gradient technique. Apodization with a shifted sine bell and baseline correction was implemented to process 2D spectra.

1D ^{1}H NMR spectra: Size 32 K, pulse length 2.8 ms (30°), 16 acquisitions.

2D COSY spectra: Sequence: D1-90-tl- G_1-90-G_2-AQ; relaxation delay D1 = 1 s, 90° pulse 8.5 μs, gradient ratio 1:1.

2D TOCSY spectra: Relaxation delay D1 = 2 s; mixing time 41.3 ms; 90° pulse 8.5 μs; TPPI-mode, NS = 64.

2D Proton-detected heteronuclear multiple quantum correlation (HMQC) experiments. Sequence: D190(^{1}H)-D2-90-(^{13}C)-t_1/2-G1-180(^{1}H)-G2-t_1/2-90(^{13}C)-G3-D2-AQ (GARP(^{13}C)), relaxation delay D1 = 2s; D2 = 3.45 ms; 90° pulse (^{1}H) 8.5 μs; 90° pulse (^{13}C) 10.5 μs, gradient ratio 5:3:4.

For DNMR spectroscopy, the probe temperature was controlled by a standard unit calibrated using a methanol reference; samples were allowed to equilibrate for 15 min at each temperature before recording spectra.

Supporting Information Available: Copies of NMR spectra (19 pages). This material is contained in libraries on microfiche, immediately follows this article in the microfilm version of the journal, can be ordered from the ACS, see any current masthead page for ordering information.

JO980029+

(11) Maple, J. R.; Dinur, U.; Hagler, A. T. *Proc. Natl. Acad. Sci. U.S.A.* **1988**, *85(15)*, 5350−5354.

(12) Cioslowski, J.; Kertesz, M. *QCPE Bull.* **1987**, *7*, 159.

(13) (a) Dewar, M. J. S.; Zoebisch, E. G.; Healy, E. F.; Stewart, J. J. P. *J. Am. Chem. Soc.* **1985**, *107*, 3902−3909. (b) Havel, T. F. *Prog. Mol. Biol. Biophys.* **1991**, *56*, 43−78. (c) Stewart, J. J. P. *J. Comput. Chem.* **1989**, *10*, 209−220. (d) Komorinski, A.; Mclver, J. W., Jr. *J. Am. Chem. Soc.* **1973**, *95*, 4512−4517.